Spectroscopic Studies of Substrate Interactions with Clavaminate Synthase 2, a Multifunctional α-KG-Dependent Non-Heme Iron Enzyme: Correlation with Mechanisms and Reactivities

Jing Zhou,[†] Wendy L. Kelly,[§] Brian O. Bachmann,[§] Michele Gunsior,[§] Craig A. Townsend,*[,§] and Edward I. Solomon*[,†]

Contribution from the Departments of Chemistry, Stanford University, Stanford, California 94305, and The Johns Hopkins University, Baltimore, Maryland 21218

Received November 20, 2000. Revised Manuscript Received May 21, 2001

Abstract: Using a single ferrous active site, clavaminate synthase 2 (CS2) activates O_2 and catalyzes the hydroxylation of deoxyguanidinoproclavaminic acid (DGPC), the oxidative ring closure of proclavaminic acid (PC), and the desaturation of dihydroclavaminic acid (and a substrate analogue, deoxyproclavaminic acid (DPC)), each coupled to the oxidative decarboxylation of cosubstrate, α-ketoglutarate (α-KG). CS2 can also catalyze an uncoupled decarboxylation of α-KG both in the absence and in the presence of substrate, which results in enzyme deactivation. Resting CS2/Fe^{II} has a six-coordinate Fe^{II} site, and α-KG binds to the iron in a bidentate mode. The active site becomes five-coordinate only when both substrate and α-KG are bound, the latter still in a bidentate mode. Absorption, CD, MCD, and VTVH MCD studies of the interaction of CS2 with DGPC, PC, and DPC provide significant molecular level insight into the structure/function correlations of this multifunctional enzyme. There are varying amounts of six-coordinate ferrous species in the substrate complexes, which correlate to the uncoupled reaction. Five-coordinate ferrous species with similar geometric and electronic structures are present for all three substrate/α-KG complexes. Coordinative unsaturation of the Fe^{II} in the presence of both cosubstrate and substrate appears to be critical for the coupling of the oxidative decarboxylation of α-KG to the different substrate oxidation reactions. In addition to the substrate orientation relative to the open coordination position on the iron site, it is hypothesized that the enzyme can affect the nature of the reactivity by further regulating the binding energy of the water to the ferrous species in the enzyme/succinate/product complex.

Introduction

Mononuclear non-heme iron enzymes catalyze a variety of important reactions involving the binding and activation of dioxygen.[1−3] Enzymes which activate O_2 in their high-spin ferrous states include extradiol dioxygenases,[4] pterin-dependent hydroxylases,[5] α-ketoglutarate (α-KG)-dependent hydroxylases (or oxygenases)[6−8] and related enzymes (including isopenicillin N synthase (IPNS)[9] and 1-aminocyclopropane-1-carboxylic acid oxidase (ACCO)[10,11]), and the Rieske-type dioxygenases.[12] Clavaminate synthase 2 (CS2) is an interesting member of the α-KG-dependent enzyme class in that it is able to catalyze three different types of reactions using a single ferrous active site: hydroxylation, oxidative ring closure, and desaturation, dependent upon substrate.[13,14]

CS2 (MW = 35 774 kDa), an isozyme isolated from clavulanic acid-producing *Streptomyces clavuligerus*, plays a central role in the construction of a strained bicyclic clavam ring structure in the biosynthesis of clavaminic acid, an advanced precursor of the potent β-lactamase inhibitor clavulanic acid.[15] This enzyme has kinetic and physical properties and sequence homology (82% identity and 87% similarity) very similar to those of its isozyme CS1 (MW = 35 347 kDa), also isolated from *S. clavuligerus*).[15,16] As shown in Figure 1, CS2 is similar to many other α-KG-dependent non-heme iron enzymes in that it catalyzes the hydroxylation of deoxyguanidinoproclavaminic acid (DGPC) to guanidinoproclavaminic acid, coupled to the oxidative decarboxylation of cosubstrate α-KG to succinate and CO_2. During this reaction, one atom of O_2 is incorporated into

[†] Stanford University.
[§] The Johns Hopkins University.

(1) Feig, A. L.; Lippard, S. J. *Chem. Rev.* **1994**, *94*, 759−805.
(2) Que, L., Jr.; Ho, R. Y. N. *Chem. Rev.* **1996**, *96*, 2607−2624.
(3) Solomon, E. I.; Brunold, T. C.; Davis, M. I.; Kemsley, J. N.; Lee, S. K.; Lehnert, N.; Neese, F.; Skulan, A. J.; Yang, Y. S.; Zhou, J. *Chem. Rev.* **2000**, *100*, 235−349.
(4) Tatsuno, Y.; Saeki, Y.; Nozaki, M.; Otsuka, S.; Maeda, Y. *FEBS Lett.* **1980**, *112*, 83−85.
(5) Shiman, R.; Gray, D. W. *J. Biol. Chem.* **1980**, *255*, 4793−4800.
(6) Prescott, A. G.; Lloyd, M. D. *Nat. Prod. Rep.* **2000**, *17*, 367−383.
(7) Kivirikko, K. I.; Myllylä, R. In *The Enzymology of Posttranslational Modification of Proteins*; Freedman, R. B., Hawkins, H. C., Eds.; Academic Press: London, 1980; Vol. 1, pp 53−104.
(8) Holme, E. *Biochemistry* **1975**, *14*, 4999−5003.
(9) Samson, S. M.; Belagaje, R.; Blankenship, D. T.; Chapman, J. L.; Perry, D.; Skatrud, P. L.; Vanfrank, R. M.; Abraham, E. P.; Baldwin, J. E.; Queener, S. W. *Nature* **1985**, *318*, 191−194.
(10) Adams, D. O.; Yang, S. F. *Proc. Natl. Acad. Sci. U.S.A* **1979**, *76*, 170−174.
(11) Abeles, F. B.; Morgan, P. W.; Saltveit, M. E. J. *Ethylene in Plant Biology*; Academic: San Diego, 1992.
(12) Ballou, D.; Batie, C. *Prog. Clin. Biol. Res.* **1988**, *274*, 211−226.
(13) Elson, S. W.; Baggaley, K. H.; Gillett, J.; Holland, S.; Nicholson, N. H.; Sime, J. T.; Woroniecki, S. R. *J. Chem. Soc., Chem. Commun.* **1987**, 1736−1740.
(14) Busby, R. W.; Townsend, C. A. *Bioorg. Med. Chem.* **1996**, *4*, 1059−1064.
(15) Salowe, S. P.; Marsh, E. N.; Townsend, C. A. *Biochemistry* **1990**, *29*, 6499−6508.
(16) Marsh, E. N.; Chang, M. D.-T.; Townsend, C. A. *Biochemistry* **1992**, *31*, 12648−12657.

10.1021/ja004025+ CCC: $20.00
Published on Web 07/10/2001

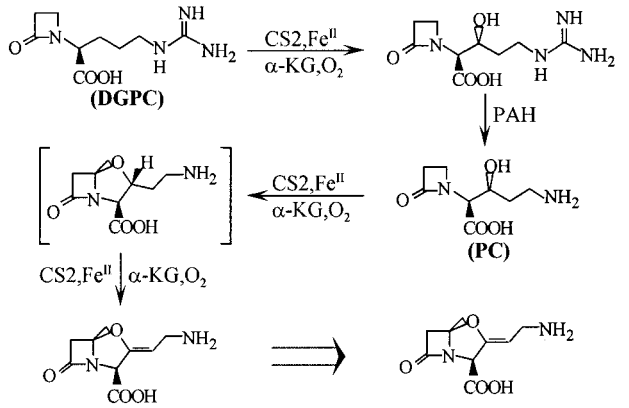

Figure 1. Biosynthetic pathway of clavulanic acid.

Scheme 1

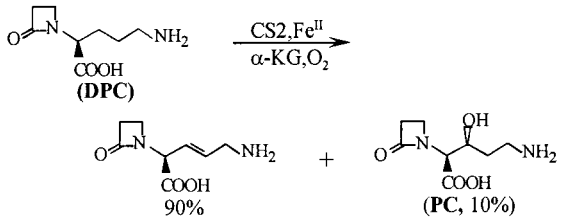

the hydroxylated product and the other appears in succinate.[17,18] Before CS2 catalyzes further reactions, proclavaminate amidino hydrolase removes the guanyl group to form proclavaminic acid (PC).[19,20] CS2 then catalyzes the oxidative ring closure of PC to dihydroclavaminic acid and its subsequent desaturation to clavaminic acid, both of which are coupled to the oxidative decarboxylation of α-KG.[13,21] In the ring-closure and desaturation reactions, the second atom of oxygen is not incorporated into the product but is reduced to water. A substrate analogue study indicated that deoxyproclavaminic acid (DPC) is converted by CS2 to a major desaturation product and a minor hydroxylation product, PC (Scheme 1).[17]

Proposed mechanisms for CS2 incorporate observed sequential kinetics and begin with the binding of Fe^{II}, α-KG, substrate, and O_2. This is followed by nucleophilic attack of the iron-bound dioxygen onto the α-keto carbon, which results in the oxidative decarboxylation of α-KG to yield succinate, CO_2, and a reactive iron−oxygen species,[15,21] proposed to be an oxo-ferryl (Fe^{IV}═O^{II-}) intermediate for other α-KG-dependent enzymes.[22−24] In the hydroxylation reaction, this reactive iron species inserts oxygen to hydroxylate DGPC substrate with retention of configuration and removal of the 3-(*pro-R*) hydrogen.[18] For the PC substrate, the 4′-(*pro-S*) hydrogen was specifically lost in the process of cyclization to the 3-OH group, which also proceeds with retention of stereochemistry.[25,26] The PC substrate has been suggested to be able to bind through the 3-OH group to the reactive iron species.[27] Earlier studies on the primary and α-secondary tritium kinetic isotope effects[21] and more recent studies of the β-secondary deuterium kinetic isotope effect[28] in the ring-closure and desaturation reactions favor a homolytic C−H abstraction by the reactive oxo-ferryl intermediate to form a carbon-centered radical (or possibly an organoiron species), resulting in the cyclization of substrate to produce dihydroclavaminate and the release of water. Thus, instead of conventional dioxygenase activity, CS2 was suggested to promote radical (or cation) capture *intra*molecularly with substrate-derived oxygen rather than *inter*molecularly with a dioxygen-derived species. In the desaturation reactions, dihydroclavaminate (the bracketed species in Figure 1) largely remains in the active site as a new oxo-ferryl species is generated from second equivalents of α-KG and O_2. Hydrogen abstraction is then proposed to occur at C-3 to form a carbon-centered radical, leading to desaturation of dihydroclavaminate to clavaminate.[21]

In the absence of substrates, an uncoupled reaction occurs in many of the α-KG-dependent enzymes but proceeds at rates significantly below those of normal substrate turnover (1−6%).[29−34] It has been proposed that, in the uncoupled reaction, the reactive oxo-ferryl species resulting from α-KG decarboxylation is quenched by water or a nearby protein ligand, thus inactivating the enzyme.[15] For prolyl 4-hydroxylase, lysyl hydroxylase,[35,36] and γ-butyrobetaine hydroxylase,[37] the uncoupled reaction is accelerated by substrate analogues that cannot be hydroxylated. For thymine hydroxylase, the uncoupled reaction occurs only in the presence of substrate analogues.[29,32] For CS2, the uncoupled reaction occurs both in the absence and in the presence of substrate (PC), but the rate in the presence of substrate is reduced to about one-third (enzyme inactivation with substrate, $t_{1/2} = 17$ min, $k = 0.04$ min^{-1}; without substrate, $t_{1/2} = 5$ min, $k = 0.14$ min^{-1}).[15]

Four X-ray crystal structures for CS1 have recently been published: the CS1/Fe^{II} complex (PDB ID 1DS0), CS1/Fe^{II}/α-KG complex (PDB ID 1DS1), CS1/Fe^{II}/α-KG/N-α-L-acetylarginine (NAA) complex (PDB ID 1DRY), and CS1/Fe^{II}/α-KG/PC complex (PDB ID 1DRT).[38] The main chain of CS1 contains a core of 10 β-strands, eight of which are folded into a distorted jellyroll structure. The jellyroll structure is sandwiched between two α-helical regions. In the CS1/Fe^{II} complex, the six-coordinate Fe^{II} ion appears in the center of the jellyroll

(17) Baldwin, J. E.; Lloyd, M. D.; Wha-Son, B.; Schofield, C. J.; Elson, S. W.; Baggaley, K. H.; Nicholson, N. H. *J. Chem. Soc., Chem. Commun.* **1993**, 500−502.
(18) Baldwin, J. E.; Merritt, K. D.; Schofield, C. J.; Elson, S. W.; Baggaley, K. H. *J. Chem. Soc., Chem. Commun.* **1993**, 1301−1302.
(19) Elson, S. W.; Baggaley, K. H.; Davidson, M.; Fulston, M.; Nicholson, N. H.; Risbridger, G. D.; Tyler, J. W. *J. Chem. Soc., Chem. Commun.* **1993**, 1211−1212.
(20) Wu, T. K.; Busby, R. W.; Houston, T. A.; McIlwaine, D. B.; Egan, L. A.; Townsend, C. A. *J. Bacteriol.* **1995**, *177*, 3714−3720.
(21) Salowe, S. P.; Krol, W. J.; Iwata-Reuyl, D.; Townsend, C. A. *Biochemistry* **1991**, *30*, 2281−2292.
(22) Siegel, B. *Bioorg. Chem.* **1979**, *8*, 219−226.
(23) Myllylä, R.; Tuderman, L.; Kivirikko, K. I. *Eur. J. Biochem.* **1977**, *80*, 349−357.
(24) Hanauske-Abel, H. M.; Günzler, V. *J. Theor. Biol.* **1982**, *94*, 421−455.
(25) Baggaley, K. H.; Nicholson, N. H.; Sime, J. T. *J. Chem. Soc., Chem. Commun.* **1988**, 567−568.
(26) Basak, A.; Salowe, S. P.; Townsend, C. A. *J. Am. Chem. Soc.* **1990**, *112*, 1654−1656.
(27) Townsend, C. A.; Basak, A. *Tetrahedron* **1991**, *47*, 2591−2602.
(28) Iwata-Reuyl, D.; Basak, A.; Townsend, C. A. *J. Am. Chem. Soc.* **1999**, *121*, 11356−11368.
(29) Thornburg, L. D.; Lai, M.-T.; Wishnok, J. S.; Stubbe, J. *Biochemistry* **1993**, *32*, 14023−14033.
(30) Tuderman, L.; Myllylä, R.; Kivirikko, K. I. *Eur. J. Biochem.* **1977**, *80*, 341−348.
(31) Puistola, U.; Turpeenniemi-Hujanen, T. M.; Myllylä, R.; Kivirikko, K. I. *Biochim. Biophys. Acta* **1980**, *611*, 40−50.
(32) Holme, E.; Lindstedt, S.; Nordin, I. *Biochem. Biophys. Res. Commun.* **1982**, *107*, 518−524.
(33) Wehbie, R. S.; Punekar, N. S.; Lardy, H. A. *Biochemistry* **1988**, *27*, 2222−2228.
(34) Hsu, C.-A.; Saewert, M. D.; Polsinelli, L. F., Jr.; Abbott, M. T. *J. Biol. Chem.* **1981**, *256*, 6098−6101.
(35) Counts, D. F.; Cardinale, G. J.; Udenfriend, S. *Proc. Natl. Acad. Sci. U.S.A.* **1978**, *75*, 2145−2149.
(36) Rao, N. V.; Adams, E. *J. Biol. Chem.* **1978**, *253*, 6327−6330.
(37) Holme, E.; Lindstedt, S. *Biochim. Biophys. Acta* **1982**, *704*, 278−283.
(38) Zhang, Z. H.; Ren, J. S.; Stammers, D. K.; Baldwin, J. E.; Harlos, K.; Schofield, C. J. *Nat. Struct. Biol.* **2000**, *7*, 127−133.

structure and has three protein ligands, His144, Glu146, and His279 (corresponding to His145, Glu147, and His280 in CS2, respectively), and three water molecules,[38] consistent with earlier spectroscopic studies on CS2 (vide infra).[39] In the CS1/Fe^{II}/α-KG complex, α-KG binds to the Fe^{II} ion through its α-keto-carboxylate moiety in a bidentate manner, replacing two coordinated water molecules,[38] which is again consistent with earlier spectroscopic results on CS2 (vide infra).[39] The remaining water molecule coordinated to the Fe^{II} occupies the position trans to His279 and cis to the plane formed by the Fe^{II} and the α-KG α-keto-carboxylate moiety.[38] A stable analogue of DGPC, *N*-α-L-acetylarginine (NAA), which lacks the 4′-C atom and thus, in contrast to DGPC, has an open *β*-lactam ring, binds in the active site pocket, positioning its guanidino group to form a major planar electrostatic interaction with the side chain of Asp233 while its carboxylate group is bound to Arg297 through a water molecule. The Fe^{II} site is still described as six-coordinate with an elongated Fe^{II}−water bond length (from 2.2 Å in the CS1/Fe^{II}/α-KG structure to 2.35 Å in the CS1/Fe^{II}/α-KG/NAA structure).[38] Alternately, spectroscopic studies on the CS2/Fe^{II}/α-KG/DGPC complex indicate a more complete conversion to a five-coordinate ferrous species.[40] The 3-(*pro-R*) C−H bond of NAA, the counterpart of which becomes oxidized in DGPC, projects toward the coordinated water in the CS1/Fe^{II}/α-KG/NAA complex. In the CS1/Fe^{II}/α-KG/PC complex, the PC substrate is located in the active site in the same general manner as NAA, except that the amino group in PC binds less rigidly than the guanidino group of NAA and that the hydroxyl group in PC is hydrogen-bonded to Ser134, thus prevented from being coordinated to Fe^{II} ion. The Fe^{II} site in the CS1/Fe^{II}/α-KG/PC complex has a five-coordinate structure.[38]

Non-heme ferrous sites have been difficult to study by spectroscopic means as these lack strong absorption features and are non-Kramers ions that are generally EPR silent. We have developed a protocol utilizing room-temperature circular dichroism (CD), low-temperature magnetic circular dichroism (MCD), and variable-temperature, variable-field (VTVH) MCD spectroscopies to probe the geometric and electronic structure of high-spin $S = 2$ Fe^{II} centers.[3,41−43] The ^5D ground state for d^6 Fe^{II} is split under octahedral symmetry into a $^5T_{2g}$ ground state (corresponding to an extra electron in d_{yz}, d_{xz}, d_{xy}) and a ^5E_g excited state (corresponding to an extra electron in $d_{x^2-y^2}$, d_{z^2}), separated by $10Dq \approx 10\,000$ cm^{-1} for biologically relevant O and N ligands. Near-IR (NIR) MCD spectroscopy allows the direct observation of the d→d transitions between the $^5T_{2g}$ ground state and the ^5E_g excited state, and the splitting of the ^5E_g excited state ($\Delta^5E_g \equiv d_{x^2-y^2} - d_{z^2}$) is sensitive to the coordination number and geometry of the site. In general, six-coordinate distorted octahedral Fe^{II} sites show two transitions at ∼10 000 cm^{-1}, split by ∼2000 cm^{-1} ($\Delta^5E_g \approx 2000$ cm^{-1}), five-coordinate sites show two transitions at ∼10 000 and ∼5000 cm^{-1} ($\Delta^5E_g \approx 5000$ cm^{-1}), and distorted four-coordinate sites show two transitions in the 4000−7000 cm^{-1} region.

VTVH MCD provides complementary ground-state electronic structure information.[3,41−43] The MCD intensity for non-Kramers Fe^{II} centers shows an unusual temperature and field dependence, which is characterized by a set of nested saturation magnetization curves (i.e., nonsuperimposed isotherms when plotted as a function of $\beta H/2kT$). For negative zero-field splitting (ZFS) systems ($D < 0$, $M_S = \pm 2$ lowest), this behavior is due to the rhombic zero-field splitting (δ) of the $M_S = \pm 2$ ground state. Ground-state spin Hamiltonian parameters are obtained by numerically fitting experimental VTVH MCD data to eq 1 in ref 44. Positive ZFS systems ($D > 0$, $M_S = 0$ lowest) show VTVH MCD behavior qualitatively similar to that of the negative ZFS systems but can be distinguished by their larger nesting, which arises from the pseudodoublet ground-state behavior of the $M_S = 0$ and one component of the $M_S = \pm 1$ sublevels (at an energy of $+D$).[42,45] The ground-state spin Hamiltonian parameters can be used to directly obtain the splitting of the $^5T_{2g}$ state ($\Delta = d_{xz,yz} - d_{xy}$ and $V = d_{xz} - d_{yz}$) and, hence, the t_{2g} orbital energies.[42] Thus, the combination of NIR MCD and VTVH MCD spectroscopies provides a complete experimental description of the d orbital energies for a given Fe^{II} site, which can be used to probe oxygen and substrate reactivity and to obtain mechanistic insight on a molecular level for non-heme iron enzymes.[3,42]

We have applied these techniques to directly probe the ferrous active site in resting CS2 and its interaction with α-KG cosubstrate as well as the DGPC substrate.[39,40] NIR CD, MCD, and VTVH MCD data show that the CS2/Fe^{II} complex contains a six-coordinate ferrous center and that addition of α-KG perturbs the site to produce a different six-coordinate center with relatively strong *π*-interactions between Fe^{II} and α-KG.[39] UV/vis absorption, CD, and MCD spectroscopic studies of the CS2/Fe^{II}/α-KG complex showed the appearance of low-lying metal-to-ligand charge-transfer (MLCT) transitions and established a bidentate binding mode of α-KG to Fe^{II},[39] which was confirmed by the later X-ray crystallographic studies on DAOCS[46] and the more recent results on CS1 (vide supra).[38] Further studies on the interaction of CS2 with DGPC substrate demonstrated that the ferrous site is converted into a five-coordinate species when both substrate, DGPC, and cosubstrate, α-KG, are bound, the latter to the Fe^{II} again in a bidentate mode.[40] The open coordination position would allow rapid O_2 reaction to generate a highly active oxygen intermediate in the proximity of bound substrates. This provided significant insight into the coupling of the oxidative decarboxylation of α-KG to the hydroxylation of the substrate and defined a general strategy utilized by a number of non-heme ferrous enzymes to generate a reactive O_2 intermediates in the presence of substrate.[3,40]

We now expand the substrate binding studies on DGPC (hydroxylation substrate) and extend them to include two other substrates, the oxidative ring-closure substrate PC and a substrate that favors the desaturation reaction to the hydroxylation reaction (DPC, >9:1). These studies allow us to probe the molecular mechanism that controls the different reactivities toward different substrates and lead to the hypothesis that the protein may regulate the reactivity of the ferrous site by affecting its affinity for coordinated water, in addition to the substrate orientation relative to the open coordination position on the iron site.

Experimental Section

Isolation of CS2 and Synthesis of Substrates. The isozyme CS2 was overexpressed and purified according to published procedures and

(39) Pavel, E. G.; Zhou, J.; Busby, R. W.; Gunsior, M.; Townsend, C. A.; Solomon, E. I. *J. Am. Chem. Soc.* **1998**, *120*, 743−753.
(40) Zhou, J.; Gunsior, M.; Bachmann, B. O.; Townsend, C. A.; Solomon, E. I. *J. Am. Chem. Soc.* **1998**, *120*, 13539−13540.
(41) Solomon, E. I.; Zhang, Y. *Acc. Chem. Res.* **1992**, *25*, 343−352.
(42) Solomon, E. I.; Pavel, E. G.; Loeb, K. E.; Campochiaro, C. *Coord. Chem. Rev.* **1995**, *144*, 369−460.
(43) Pavel, E. G.; Kitjima, N.; Solomon, E. I. *J. Am. Chem. Soc.* **1998**, *120*, 3949−3962.
(44) Pavel, E. G.; Kitajima, N.; Solomon, E. I. *J. Am. Chem. Soc.* **1998**, *120*, 3949−3962.
(45) Campochiaro, C.; Pavel, E. G.; Solomon, E. I. *Inorg. Chem.* **1995**, *34*, 4669−4675.
(46) Valegård, K.; Vanscheltinga, A. C. T.; Lloyd, M. D.; Hara, T.; Ramaswamy, S.; Perrakis, A.; Thompson, A.; Lee, H. J.; Baldwin, J. E.; Schofield, C. J.; Hajdu, J.; Andersson, I. *Nature* **1998**, *394*, 805−809.

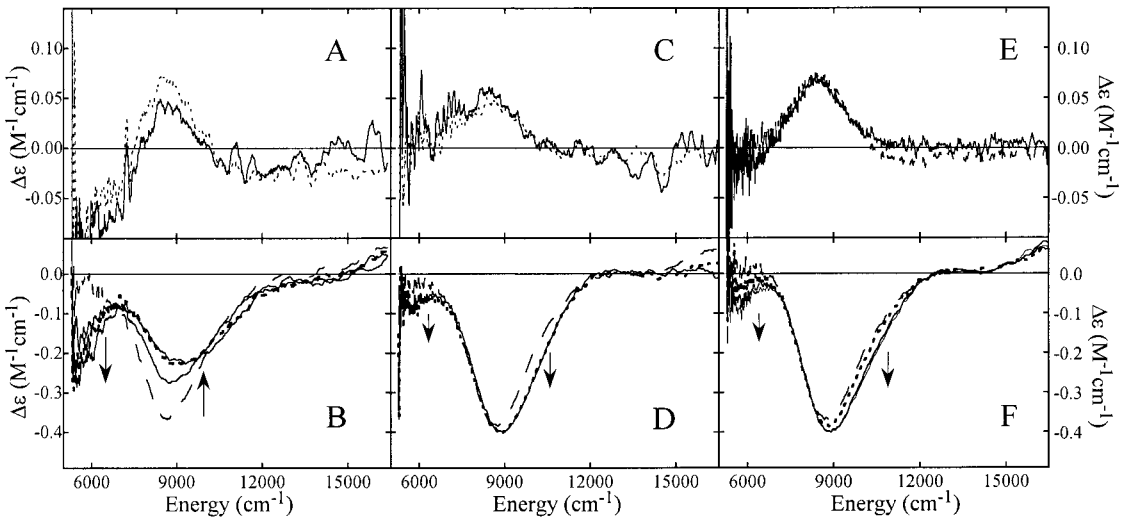

Figure 2. Near-IR CD titration studies of substrate binding to CS2/Fe^{II}. (A) DGPC titration in the absence of α-KG. Solid line, CS2/Fe^{II}; dotted line, CS2/Fe^{II} with 1.5 equiv of DGPC. (B) DGPC titration to CS2/Fe^{II}/α-KG. DGPC added is 0, 0.5, 1.0 (thick dashed line), and 1.5 equiv relative to CS2/Fe^{II}/α-KG. (C) PC titration to CS2/Fe^{II} in the absence of α-KG. Solid line, CS2/Fe^{II}; dotted line, CS2/Fe^{II} with 2 equiv of PC. (D) PC titration of CS2/Fe^{II}/α-KG. PC added is 0, 1.0 (thick dashed line), and 2.0 equiv relative to CS2/Fe^{II}/α-KG. (E) DPC titration to in the absence of α-KG. Solid line, CS2/Fe^{II}; dotted line, CS2/Fe^{II} with 8 equiv of DPC. (C) DPC titration to CS2/Fe^{II}/α-KG. DPC added is 0, 1.0 (dashed line), 4.0, and 8.0 equiv relative to CS2/Fe^{II}/α-KG. Note: Data have been smoothed to clearly distinguish the low-energy band at ∼5000 cm^{-1}. The low-energy bands at ∼5000 cm^{-1} in the spectra are cut off due to solvent at ∼1900 nm (∼5260 cm^{-1}).

modifications.[39,47] The substrates DGPC, DPC, and PC were synthesized as previously described.[20,21]

Preparation of Samples for Spectroscopy. All commercial reagents were used without further purification: MOPS buffer (Sigma), D_2O (99.9 atom % D; Aldrich), sodium deuterioxide (99+ atom % D; Sigma), glycerol-d_3 (98 atom % D; Cambridge Isotopes Laboratory), α-ketoglutaric acid (2-oxopentanedioic acid) sodium salt (Sigma), and ferrous ammonium sulfate (FeAS, $[Fe(H_2O)_6](NH_4)_2(SO_4)_2$; MCB Manufacturing Chemists, Inc.). All samples for spectroscopy were prepared under an inert atmosphere inside a N_2-purged wet box. ApoCS2 was made anaerobic by purging the apoenzyme with argon gas on a Schlenk line and alternating quick cycles of vacuum and argon. Fe^{II}, α-KG, and substrates were added in microliter quantities from anaerobic stock solutions of Fe^{II}, α-KG, and substrates in degassed MOPS buffer, pD 7, respectively. Fresh stock solutions for Fe^{II} and α-KG were prepared for each set of experiments. For substrates, stock solutions were made anaerobic by ∼20 times of freeze−pump−thaw on a Schlenk line every time before use. CS2/Fe^{II} samples contain 0.8 equiv of Fe^{II} relative to apoenzyme, and CS2/Fe^{II}/α-KG samples had 15 equiv of α-KG relative to apoenzyme.

Samples for absorption and CD spectroscopy (2.5−4.5 mM apoCS2) were kept anaerobic in a custom-made 0.5-cm-path length masked optical cell (Wilmad) fitted with a gastight Teflon stopcock (LabGlass). Titration additions into the anaerobic optical cell were carried out in the wet box using gastight syringes fitted with custom 5-in.-long needles (Hamilton Co.); volumes were adjusted to account for the added solution. Samples for MCD spectroscopy (1.0−2.0 mM apoCS2) were prepared by the anaerobic addition of FeAS to the apoenzyme, followed by addition of α-KG where appropriate, and 55−65 vol % of degassed glycerol-d_3. MCD samples were injected into a cell with a 0.3-cm-thick neoprene spacer sandwiched between two infrasil quartz disks and secured between two copper plates; cells were frozen under liquid N_2 immediately upon removal from the wet box.

Instrumentation. NIR (600−2000 nm) CD and MCD spectra were recorded on a Jasco J200D spectropolarimeter with a liquid N_2-cooled InSb detector and an Oxford Instruments SM4000-7T superconducting magnet/cryostat (0−7 T, 1.5−300 K). UV/vis (300−850 nm) CD and MCD spectra were obtained on a Jasco J500C spectropolarimeter with an extended S-20 photomultiplier tube (Hammamatsu) and equipped with an Oxford Instruments SM4-7T magnet/cryostat capable of fields up to 7 T and temperatures from 1.5 to 300 K. Room-temperature UV/vis (190−820 nm) electronic absorption spectra were recorded on an HP 8452A diode array spectrophotometer.

CD samples were maintained at a temperature of 278 K using a recirculating water bath and thermostatic cell holder (HP) on each spectropolarimeter. CD spectra are baseline corrected by subtracting the buffer and cell backgrounds from the raw data. Depolarization of frozen MCD samples was judged to be <5% by comparing the CD spectra of a nickel (+)-tartrate solution placed before and after the sample. The reported MCD spectra and the VTVH MCD data are the averaged subtraction of the negative field raw data from the positive field raw data so as to avoid subtraction problems due to shifting baselines in poor quality frozen glasses.

Fitting Procedures. Saturation magnetization data were normalized to the maximum observed intensity and fit according to published procedures to extract ground-state parameters.[42] Both the negative and positive ZFS models were applied to the VTVH MCD data in determining the best fit. Binding constants were estimated from CD titration data using the method of Rose and Drago.[48]

Results and Analysis

A. NIR CD Titrations of Substrate Binding. CD spectroscopy has been used to probe substrate binding to CS2/Fe^{II} both in the presence and in the absence of the cosubstrate α-KG and to estimate binding constants.

1. In the Absence of α-KG. The dotted line in Figure 2A (and Figure 2C,E) shows the NIR CD spectrum of CS2/Fe^{II} at 278 K prior to addition of substrate or cosubstrate. This has a very weak and broad positive asymmetric composite band assigned as d→d transitions of Fe^{II} bound at the active site in the resting CS2/Fe^{II} complex.[39] Addition of DGPC, PC, or DPC to this CS2/Fe^{II} complex in the absence of α-KG results in no change of the CD spectrum (solid line in Figure 2A, C, and E, respectively). This indicates that in the absence of α-KG, either DGPC, PC, or DPC substrate does not bind to the CS2/Fe^{II} complex or the binding does not affect the iron site.

2. In the Presence of α-KG. The dashed line in Figure 2B (and Figure 2D,F) shows the NIR CD spectrum of the

(47) Busby, R. W.; Chang, M. D.-T.; Busby, R. C.; Wimp, J.; Townsend, C. A. *J. Biol. Chem.* **1995**, *270*, 4262−4269.

(48) Connors, K. A. *Binding Constants: The Measurement of Molecular Complex Stability*; John Wiley & Sons: New York, 1987; Chapter 4.

Table 1. Ligand Field MCD Transition Energies, Ground-State Spin Hamiltonian Parameters, and Ligand Field Parameters

		CS2/Fe^{II}/α-KG/DGPC			CS2/Fe^{II}/α-KG/PC			CS2/Fe^{II}/α-KG/DPC	
peak positions energy splitting		∼520, 8800 cm^{-1} 3600 cm^{-1}			∼5200, 8600 cm^{-1} 3400 cm^{-1}			∼5200, 8600 cm^{-1} 3400 cm^{-1}	
VTVH positions		6060 cm^{-1}	8500 cm^{-1}	10 000 cm^{-1}	6060 cm^{-1}	8140 cm^{-1}	9200 cm^{-1}	8000 cm^{-1}	9600 cm^{-1}
$-D$	δ (cm^{-1})	2.1 ± 0.2	2.1 ± 0.2		1.9 ± 0.2	1.9 ± 0.2		1.8 ± 0.3	
	$g_{\|\|}$	8.8 ± 0.2	8.8 ± 0.2		8.8 ± 0.2	8.8 ± 0.2		8.9 ± 0.2	
	M_z/M_{xy}[a]	−0.2	−0.3		0.1	−0.2		0.1	
	B term[b]	−0.2	1.7		0.1	0.7		0.6	
$+D$	D (cm^{-1})			9 ± 0.2			6 ± 0.2		7 ± 0.2
	$\|E\|$ (cm^{-1})			1 ± 0.1			1 ± 0.1		1.4 ± 0.1
Δ (cm^{-1})		−1300 ± 250		750 ± 100	−1250 ± 250		1000 ± 100	−1250 ± 250	1000 ± 100
$\|V/2\Delta\|$		0.27 ± 0.05		0.13 ± 0.02	0.25 ± 0.05		0.18 ± 0.02	0.25 ± 0.05	0.23 ± 0.02
$\|V\|$ (cm^{-1})		800 ± 300		200 ± 100	700 ± 300		400 ± 100	700 ± 300	450 ± 100

[a] For $g_\perp$ fixed at 1.0. [b] Reported as a percentage of the *C*-term intensity scaling factor (see ref 42).

CS2/Fe^{II}/α-KG (5 equiv) complex, which contains a broad negative band associated with the d→d transitions of a six-coordinate Fe^{II} with α-KG coordinated in a bidentate mode at the active site in the CS2/Fe^{II}/α-KG complex.[39]

Addition of increasing aliquots of either DGPC, PC, or DPC substrate to the CS2/Fe^{II}/α-KG complex results in the appearance of a new low-energy band at ∼5000 cm^{-1} (solid lines in Figure 2B, D, and F). In the case of DGPC, the high-energy band shifts to higher energy and decreases in intensity. The changes saturate at 1 (Figure 2B, dark dotted line)−1.5 equiv, from which an estimated binding constant of K_B > 5000 M^{-1} is obtained for DGPC binding to CS2/Fe^{II}/α-KG. This is consistent with steady-state kinetic studies which give K_m-(DGPC) = 250 ± 25 μM.[17] For PC and DPC substrate, the high-energy band in the NIR CD shifts to higher energy and increases somewhat in intensity (Figure 2D,F). These changes saturate at 1 (dark dotted line in Figure 2D)−2 equiv for PC, and an equilibrium constant for PC binding in the CS2/Fe^{II}/α-KG/PC complex is estimated to be K_B (PC) > 1000 M^{-1}, again consistent with steady-state kinetic results (K_m(PC) = 440 μM).[49] For DPC, the changes saturate at 4−8 equiv (Figure 2F), indicating a weaker binding interaction for this non-natural substrate to the enzyme (estimated K_B(DPC) > 200 M^{-1}). The changes for PC and DPC are smaller than those for DGPC but are reproducible.

The completely converted species for all three substrates has a low-energy NIR CD transition at ∼5000 cm^{-1} and a high-energy transition (∼8600 cm^{-1} for DGPC, Figure 2B dark dotted line; ∼9000 cm^{-1} for PC and DPC substrates, Figure 2D,F dark dotted line), indicating the presence of a 5C Fe^{II} site in all three CS2/Fe^{II}/α-KG/substrate complexes.

Further addition of cosubstrate α-KG up to 10 equiv does not change the spectrum of all of the above CS2/Fe^{II}/α-KG/substrate complexes, suggesting that the spectral changes are also saturated relative to the cosubstrate α-KG. Further, identical spectra are obtained from the addition of α-KG to the three CS2/Fe^{II} substrate complexes, indicating that formation of all three CS2/Fe^{II}/α-KG/substrate complexes is independent of the order of substrate/cosubstrate addition. Addition of 60% (v/v) glycerol-d_3 does not alter the above CD spectra; thus, glycerol may be used as a glassing agent for low-temperature MCD spectroscopy.

B. NIR MCD and VTVH MCD. The NIR MCD and VTVH MCD data for DGPC, PC, and DPC substrate binding to the CS2/Fe^{II}/α-KG complex are shown in Figures 3−5, respectively. The excited-state transition energies, ground-state splitting, and ligand field parameters for three CS2/Fe^{II}/α-KG/substrate complexes are summarized in Table 1.

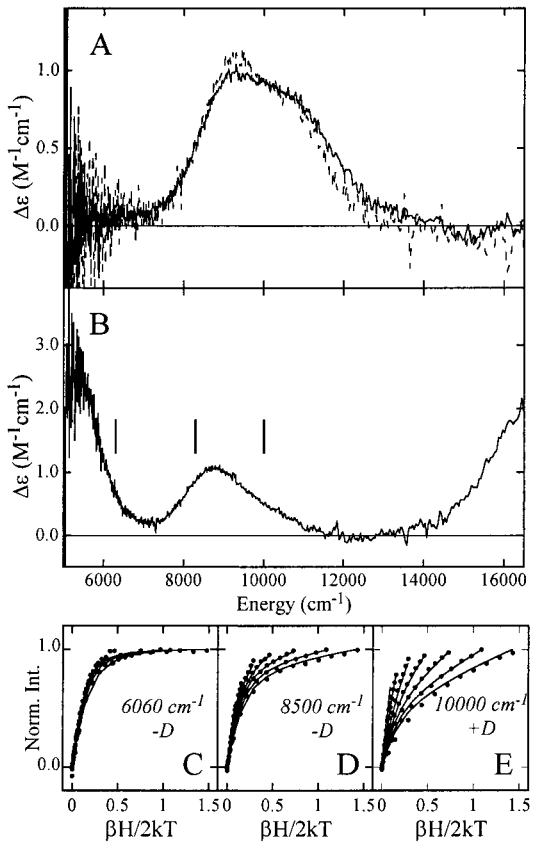

Figure 3. Near-IR MCD studies of DGPC binding to CS2. (A) MCD at 5 K, 7 T of CS2/Fe^{II} prior to (dashed line) and after (1.5 equiv, solid line) the addition of DGPC substrate in the absence of α-KG. (B) MCD at 5 K, 7 T of the CS2/Fe^{II}/α-KG/DGPC (1.5 equiv) complex. Verticle bars indicate the energy positions where the VTVH MCD data for plots C, D, and E were collected (from low to high energy, respectively). (C, D, E) VTVH MCD data (symbols) and their best fit (lines) for the CS2/Fe^{II}/α-KG/DGPC (1.5 equiv) complex collected at 6060 (C), 8500 (D), and 10 000 cm^{-1} (E).

The 5 K, 7 T MCD spectrum of resting CS2/Fe^{II} (dashed line) and that of CS2/Fe^{II} in the presence of substrate (solid line) are shown in Figure 3A for DGPC, Figure 4A for PC, and Figure 5A for DPC. In the absence of α-KG, addition of the substrate DGPC, PC, or DPC does not change the MCD

(49) Lawlor, E. J.; Elson, S. W.; Holland, S.; Cassels, R.; Hodgson, J. E.; Lloyd, M. D.; Baldwin, J. E.; Schofield, C. J. *Tetrahedron* **1994**, *50*, 8737−8748.

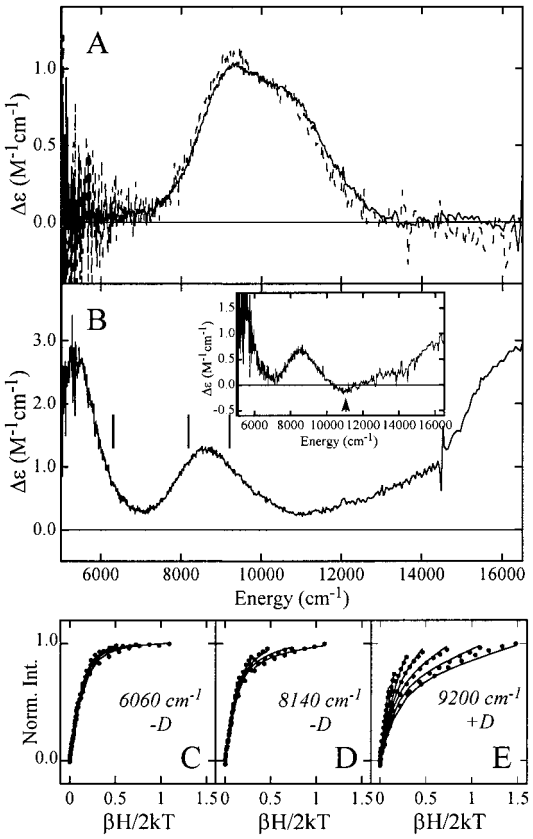

Figure 4. Near-IR MCD studies of PC binding to CS2. (A) MCD at 5 K, 7 T of CS2/Fe^{II} prior to (dashed line) and after (2 equiv, solid line) the addition of PC substrate in the absence of α-KG. (B) MCD at 5 K, 7 T of the CS2/Fe^{II}/α-KG/PC (2 equiv) complex. Vertical bars indicate the energy positions where the VTVH MCD data for plots C, D, and E were collected (from low to high energy, respectively). Inset: Low-field (2 T) MCD at 5 K of the CS2/Fe^{II}/α-KG/PC (2 equiv) complex indicating the negative feature at ∼11 000 cm^{-1} (arrow). (C, D, E) VTVH MCD data (symbols) and their best fit (lines) for the CS2/Fe^{II}/α-KG/PC (2 equiv) complex collected at 6060 (C), 8140 (D), and 9200 cm^{-1} (E).

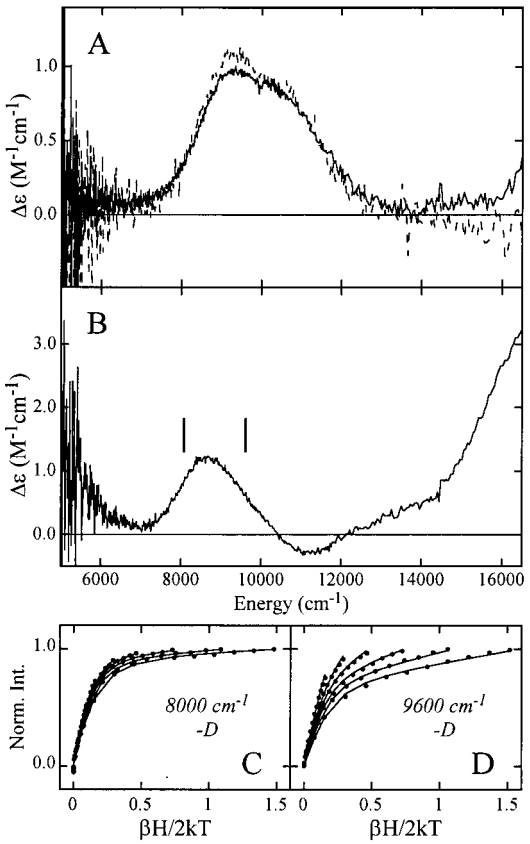

Figure 5. Near-IR MCD studies of DPC binding to CS2. (A) MCD at 5 K, 7 T of CS2/Fe^{II} prior to (dashed line) and after (8 equiv, solid line) the addition of DPC in the absence of α-KG. (B) MCD at 5 K, 7 T of the CS2/Fe^{II}/α-KG/DPC (8 equiv) complex. Vertical bars indicate the energy positions where the VTVH MCD data for plots C and D are collected (from low to high energy). (C, D) VTVH MCD data (symbols) and their best fit (lines) for the CS2/Fe^{II}/α-KG/DPC (8 equiv) complex collected at 8000 (C) and 9600 cm^{-1} (D).

spectrum of the CS2/Fe^{II} species, indicating that either the substrate does not bind or its binding has no effect on the iron site, consistent with the CD studies (vide supra).

1. NIR MCD of Substrate/α-KG Complexes. The 5 K, 7 T MCD spectra of the CS2/Fe^{II}/α-KG (5 equiv)/DGPC (1.5 equiv), PC (2 equiv), and DPC (8 equiv) complexes are presented in Figures 3B, 4B, and 5B, respectively. All of them contain at least two bands, one at low energy, ∼5200 cm^{-1}, and one at high energy, 8800 (DGPC complex) or 8600 cm^{-1} (PC and DPC complexes) (see Table 1). The presence of an ∼5000 cm^{-1} transition combined with a transition in the ∼9000 cm^{-1} region indicate that there is a five-coordinate Fe^{II} site in all three substrate complexes. Consistent with CD studies, further addition of α-KG and substrate does not change the MCD spectra. The asymmetric band shape of the high-energy band in the spectra implies that there is more than one species contributing to its intensity for all three substrate complexes, especially on the higher energy side. Subtraction of the MCD spectrum of the resting CS2/Fe^{II} complex or the CS2/Fe^{II}/α-KG complex from the MCD spectra of the CS2/Fe^{II}/α-KG/substrate complexes does not improve the band shape, suggesting that the asymmetric shape of the high-energy band does not derive from an unconverted component of either of these species. The inset of Figure 4B presents the MCD spectrum of the CS2/Fe^{II}/α-KG/PC complex at 5 K and 2 T, showing a negative feature (indicated with an arrow) at ∼11 000 cm^{-1}. This negative feature is not observed in the 5 K, 7 T MCD spectrum and reflects the fact that the intensity of the positive band at ∼9500 cm^{-1} has a different saturation behavior (vide infra) which overcomes the intensity of the weak negative band at higher magnetic field. This negative feature further requires that there is more than one species contributing to the MCD intensity in this energy region. This nagative feature is clearly present at 11 300 cm^{-1} for the DPC complex (Figure 5B), again indicating the presence of more than one species. The low-energy band at ∼5200 cm^{-1} for the CS2/Fe^{II}/α-KG/DPC complex has about one-third of the intensity of the corresponding low-energy band in the MCD spectra of both the CS2/Fe^{II}/α-KG/DGPC and the CS2/Fe^{II}/α-KG/PC complexes. This could have two possible origins: (1) the low-energy band could be shifted to lower energy which would decrease the intensity at ∼5200 cm^{-1}, or (2) the amount of five-coordinate species could be lower in the CS2/Fe^{II}/α-KG/DPC complex than in the CS2/Fe^{II}/α-KG/DGPC and CS2/Fe^{II}/α-KG/PC complexes. Spectral simulation indicates that only the latter will reproduce the band shape, which suggests that the addition of DPC substrate results in a lower conversion to the five-coordinate ferrous species.

2. NIR VTVH MCD of Substrate/α-KG Complexes. VTVH MCD was used to probe the ground-state splittings of the five-coordinate species in the substrate complexes by monitoring the MCD intensity at the low-energy band. It could then be used to characterize the species contributing to the high-energy MCD band by monitoring the MCD intensity at both

the higher-energy and the lower-energy sides of the high-energy band. Figures 3C−E, 4C−E, and 5C,D show these data (symbols) plotted vs $\beta H/2kT$ along with the best fit (lines) to the data for the DGPC, PC, and DPC complexes, respectively. As seen from these plots, the MCD intensity decreases with increasing temperature, indicative of a high-spin Fe^{II} center. Importantly, the data show different nesting behavior for the different positions in the spectrum (larger nesting at higher energy), confirming that more than one species contributes to the intensity of the high-energy band.

The saturation magnetization behavior for the five-coordinate species in both the DGPC complex (Figure 3C) and the PC complex (Figure 4C) could be obtained directly by monitoring the low-energy band at 6060 cm^{-1}. This is well described by the negative ZFS non-Kramers model (see Table 1 for ground-state spin Hamiltonian parameters). The value of δ is within the range expected for a five-coordinate site. Based on these parameters, the ground state $^5T_{2g}$ splittings are determined (Table 1). The saturation magnetization behavior monitored on the lower-energy side of the high-energy band at 8500 cm^{-1} for the DGPC complex (Figure 3D) and at 8140 cm^{-1} for the PC complex (Figure 4D) could be fit by the negative ZFS non-Kramers model with the same ground-state spin Hamiltonian parameters as those of the low-energy band but with different values of M_z/M_{xy} and the B term (see Table 1). For the DPC complex, the low-energy band is too low in intensity to obtain reliable VTVH MCD data. The VTVH data taken at 8000 cm^{-1} (Figure 5C) are almost superimposable (little nesting), and the saturation magnetization behavior is well described by the negative ZFS non-Kramers model (see Table 1 for ground-state spin Hamiltonian parameters), which are very similar to those obtained from the low-energy band (∼5200 cm^{-1}) associated with the five-coordinate species of the DGPC and PC complexes. Thus, from the CD, MCD, and VTVH MCD data, all three CS2/Fe^{II}/α-KG/substrate complexes contain a major component with a high-spin ferrous active site with a similar five-coordinate distorted square pyramidal geometry.

On the other hand, the saturation magnetization behavior on the higher-energy side of the high-energy band for DGPC (at 10 000 cm^{-1}, Figure 3E), PC (at 9200 cm^{-1}, Figure 4E; note that the negative feature at ∼11 000 cm^{-1} is too weak to resolve reliable VTVH MCD data), and DPC complexes (at 9600 cm^{-1}, Figure 5D) shows in all cases a large nesting which could not be fit with the negative ZFS non-Kramers model. Fitting to a positive ZFS non-Kramers model gives the result in Table 1, where the D value is large, which corresponds to a smaller splitting of $^5T_{2g}$, indicating that a six-coordinate component is also present in each complex.

Thus, the energy position and the saturation magnetization behavior of the intensity on the higher-energy side of the high-energy band indicate that a minor (∼5%) six-coordinate ferrous species is present in the DGPC complex in addition to the five-coordinate species. The six-coordinate component is also present in the PC complex and is more clearly observed by the small negative feature in the low-temperature MCD spectrum at low magnetic field for the PC complex (inset, Figure 4B). The amount of six-coordinate component present is larger than that in the DGPC complex (from the more unsymmetrical band shape of the higher-energy NIR MCD band and the more visible negative feature in the low-field MCD spectrum; this is estimated at ∼10%). The six-coordinate species is even more significant in the DPC complex (from the significant negative feature at ∼11 000 cm^{-1} in Figure 5B). Assuming the five-coordinate ferrous species have similar low-energy bands, the amount of the five-coordinate species present for the three substrate complexes are ∼95% for DGPC, ∼90% for PC, and 50% for DPC. Thus, less five-coordinate and more six-coordinate component is present for the DPC substrate α-KG complex relative to the DGPC and PC CS2/Fe^{II}/α-KG complexes.

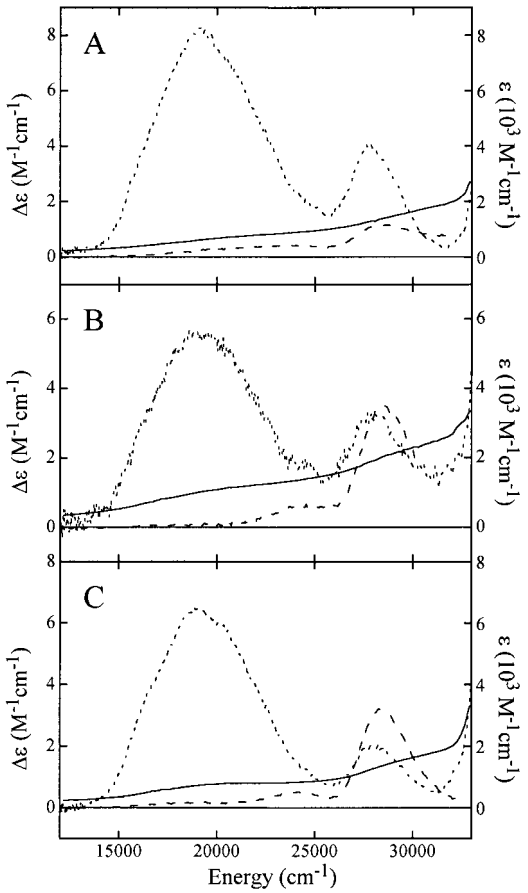

Figure 6. UV/vis abs, CD, and MCD studies of CS2/Fe^{II}/α-KG substrate complexes. (A) Abs at 298 K (solid line), CD at 298 K (dashed line), and MCD at 5 K, 7 T (dotted line) of the CS2/Fe^{II}/α-KG/DGPC (1.5 equiv) complex. (B) Abs at 298 K (solid line), CD at 298 K (dashed line), and MCD at 5 K, 7 T (dotted line) of the CS2/Fe^{II}/α-KG/PC (2 equiv) complex. (C) Abs at 298 K (solid line), CD at 298 K (dashed line), and MCD at 5 K, 7 T (dotted line) of the CS2/Fe^{II}/α-KG/DPC (4 equiv) complex.

C. UV/Vis Abs, CD, and MCD of the CS2/Fe^{II}/α-KG/Substrate Complexes. From our earlier studies on the CS2/Fe^{II}/α-KG complex, α-KG is bound in a bidentate mode through its α-keto carboxylate moiety.[39] This results in low-lying Fe^{II}-to-α-KG MLCT transitions and α-KG n→π^* transitions in the visible and near-UV spectral regions, which contain information about the interaction of the α-KG cosubstrate with the Fe^{II} ion. The effects of the three substrates binding to the CS2/Fe^{II}/α-KG complex on these spectral features were studied using UV/vis absorption, CD, and MCD spectroscopies and are summarized in Figure 6.

The solid lines in Figure 6A−C show the 278 K absorption spectra for the CS2/Fe^{II}/α-KG/DGPC, CS2/Fe^{II}/α-KG/PC, and CS2/Fe^{II}/α-KG/DPC complexes, respectively. There are two transitions, one broad band centered around 20 000 cm^{-1} (500 nm) and another band at ∼28 500 cm^{-1} (350 nm). These are more clearly observed in the CD (dashed lines) and MCD (dotted lines) spectra. The CD spectra for the three complexes show a weak broad band with a gradual increase in intensity above 13 000 cm^{-1}, a peak at 24 500 cm^{-1}, and a relatively

narrow strong band at 28 500 cm^{-1}. The MCD spectra at 5 K, 7 T for all three complexes contain a broad intense peak centered around 20 000 cm^{-1} and another band at ~28 000 cm^{-1}. The band at 20 000 cm^{-1} in the CS2/Fe^{II}/α-KG complex has been assigned as an Fe^{II}-to-α-KG MLCT transition.[39] MLCT intensity requires direct orbital overlap, thus α-KG binding to the Fe^{II} center. From model studies,[50−52] the MLCT spectrum of the CS2/Fe^{II}/α-KG complex requires that α-KG binds in a bidentate mode.[39] The fact that these transitions remain at virtually the same energy with similar intensities for all three substrates demonstrates that the cosubstrate α-KG remains bound to Fe^{II} in a bidentate mode in all three substrate active site complexes.

Discussion

α-KG-dependent non-heme iron enzymes activate dioxygen for direct hydroxylation or oxidation of substrate with the coupled oxidative decarboxylation of cosubstrate α-KG. Some members of the class of α-KG-dependent enzymes can catalyze different oxidation reactions for different substrates. Thymine 7-hydroxylase catalyzes three consecutive oxidative reactions of thymine to 5-hydroxymethylruacil, 5-formyl uracil, and uracil-5-carboxylic acid.[8,29] Deacetoxycephalosporin C synthase catalyzes two consecutive reactions in the biosynthesis of antibiotic cephalosporin: ring expansion and hydroxylation.[53] CS2 is able to catalyze three nonsuccessive different types of reactions: hydroxylation of DGPC, oxidative ring closure of PC, and desaturation of dihydroclavaminic acid and DPC.[13,18,54] This makes CS2 an appropriate system for studies directed toward understanding structure/reactivity correlations for this class of enzymes. We have addressed this through the use of CD, MCD, and VTVH MCD spectroscopies to study the geometric and electronic structure of the active site complexes formed with DGPC, PC, and DPC substrates.

NIR CD titrations at 5 °C show that in the absence of cosubstrate α-KG, either the three substrates do not bind to the enzyme or their binding has no effect on the ferrous site. However, in the presence of α-KG, all three substrates bind to the enzyme at the active site, converting the Fe^{II} from six- to five-coordinate as reflected by the appearance of a low-energy ligand field band at ~5000 cm^{-1}. The binding constants for DGPC and PC estimated from the titration studies are consistent with steady-state kinetic results. The low-temperature ligand field MCD spectra (5 K, 7 T) of the CS2/Fe^{II}/α-KG/DGPC, CS2/Fe^{II}/α-KG/PC, and CS2/Fe^{II}/α-KG/DPC complexes and VTVH MCD studies demonstrate that all three five-coordinate ferrous sites are very similar. The MLCT and $n\rightarrow\pi^*$ transitions in the UV/vis absorption, CD, and MCD spectra demonstrate that α-KG remains bound to Fe^{II} in a bidentate binding mode. In the case of the CS2/Fe^{II}/α-KG/PC complex, this excludes the possibility of the direct binding of the substrate-derived hydroxyl group to Fe^{II}. In addition to the five-coordinate ferrous species, MCD and VTVH MCD studies of these three complexes indicate that there are variable amounts of a six-coordinate ferrous species present when substrate is bound. The amount of six-coordinate component is ~5% in the hydroxylation substrate DGPC complex, is ~10% in the oxidative ring-closure substrate PC, and approaches 50% in the desaturation substrate DPC complex.

Structural Model for the Six- to Five-Coordination Conversion. The conversion from a resting six-coordinate ferrous species to a five-coordinate ferrous species in the presence of substrate (and cosubstrate) has been observed for a number of the non-heme iron enzymes, and a general mechanistic strategy for dioxygen activation by ferrous sites has been proposed.[3,40] The six-coordinate ferrous site is coordinatively saturated and fairly stable in the presence of O_2. Upon substrate (and cosubstrate) binding, the five-coordinate ferrous site provides an open coordination position for the dioxygen to interact with the iron site to generate a highly reactive iron−oxygen intermediate for the direct hydroxylation (or oxidation) of substrate (and cosubstrate). A survey of the mononuclear non-heme enzymes with available X-ray crystal structures[38,46,55−58] indicates that the conversion of a six-coordinate iron site to a five-coordinate iron site generally involves the loss of a coordinated water molecule upon substrate (and cosubstrate) binding (Figure 7). For IPNS, a water molecule bound to the metal ion trans to Asp216 is lost upon ACV binding with its thiolate directly coordinated to the metal (Figure 7A,B).[55,56] Although the structure with both the substrate and cosubstrate bound is not available for DAOCS, parallel to CS2 (vide infra), it is anticipated that the only water molecule coordinated to the ferrous ion in the cosubstrate-bound form[46] (Figure 7C) will be lost upon substrate binding. For the pterin-dependent phenylalanine hydroxylase, there are three coordinated water molecules in the resting and cosubstrate analogue-bound forms (the iron is in the ferric state).[57,58] It is reasonable to propose that one of the three coordinated water molecules is lost when both the cosubstrate and substrate are bound (MCD studies on phenylalanine hydroxylase show a six- to five-coordinate conversion).[59] For CS1, with both α-KG and the DGPC substrate analogue NAA bound, a water molecule trans to His279 is at a longer distance from the iron than that in the structure with only α-KG bound (2.35 vs 2.20 Å) (Figure 7D,E).[38] This water molecule is, in fact, lost in the structure with both α-KG and the PC substrate bound (Figure 7F).[38]

It is important to consider the structural reasons for loss of water upon substrate (and cosubstrate) binding. For IPNS, it was suggested that the presence of the hydrophobic valine side chain from substrate ACV at the position trans to Asp216 prevents the water molecule from binding.[56] Examination of the environment of the coordinated waters suggests that there are additional interactions that help stabilize their binding to the ferrous center (see Figure 7). In the structure of resting IPNS, two coordinated waters are connected to surrounding cluster of water molecules by hydrogen bonds. When substrate ACV binds, the hydrophobic valine side chain excludes the two water molecules that helped stabilize the coordinated water trans to Asp216. In contrast, the coordinated water trans to His214 remains bound to the metal ion and maintains its water cluster.

In addition to the surrounding water cluster, there is a hydrogen-bonding interaction with the uncomplexed carboxylate

(50) Chiou, Y.-M.; Que, L., Jr. *J. Am. Chem. Soc.* **1992**, *114*, 7567−7568.
(51) Chiou, Y.-M.; Que, L., Jr. *J. Am. Chem. Soc.* **1995**, *117*, 3999−4013.
(52) Ha, E. H.; Ho, R. Y. N.; Kisiel, J. F.; Valentine, J. S. *Inorg. Chem.* **1995**, *34*, 2265−2266.
(53) Baldwin, J. E.; Abraham, E. *Nat. Prod. Rep.* **1988**, *5*, 129−145.
(54) Krol, W. J.; Basak, A.; Salowe, S. P.; Townsend, C. A. *J. Am. Chem. Soc.* **1989**, *111*, 7625−7627.
(55) Roach, P. L.; Clifton, I. J.; Fülöp, V.; Harlos, K.; Barton, G. J.; Hajdu, J.; Andersson, I.; Schofield, C. J.; Baldwin, J. E. *Nature* **1995**, *375*, 700−704.
(56) Roach, P. L.; Clifton, I. J.; Hensgens, C. M. H.; Shibata, N.; Schofield, C. J.; Hajdu, J.; Baldwin, J. E. *Nature* **1997**, *387*, 827−830.
(57) Erlandsen, H.; Fusetti, F.; Martínez, A.; Hough, E.; Flatmark, T.; Stevens, R. C. *Nat. Struct. Biol.* **1997**, *4*, 995−1000.
(58) Erlandsen, H.; Bjorgo, E.; Flatmark, T.; Stevens, R. C. *Biochemistry* **2000**, *39*, 2208−2217.
(59) Kemsley, J. N.; Mitic, N.; Loeb Zaleski, K.; Caradonna, J. P.; Solomon, E. I. *J. Am. Chem. Soc.* **1999**, *121*, 1528−1536.

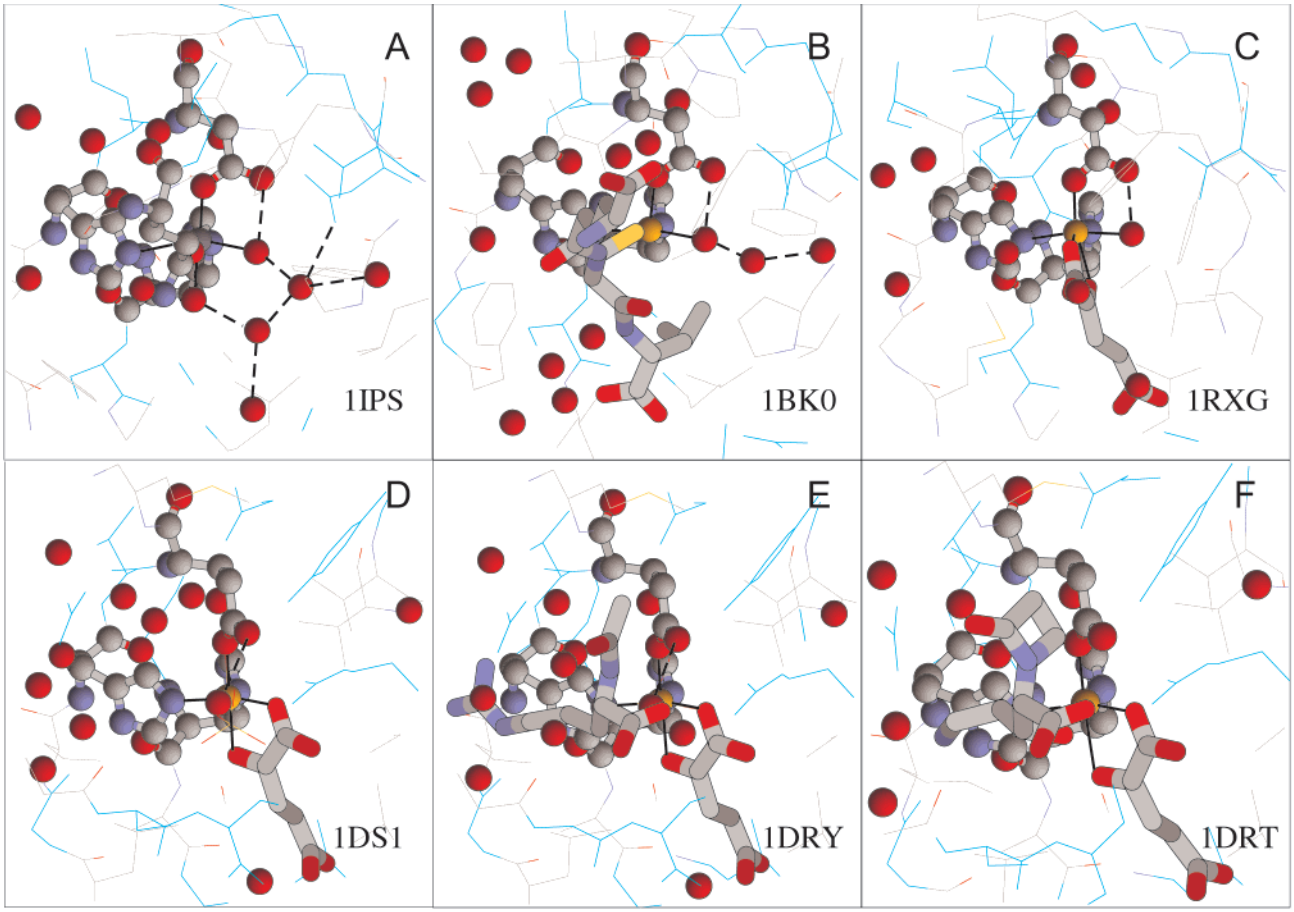

Figure 7. Active site X-ray crystal structures of some mononuclear non-heme iron enzymes. (A) Mn^{II}-substituted resting IPNS; (B) ACV-bound IPNS; (C) α-KG-bound DAOCS; (D) α-KG-bound CS1; (E) α-KG- and NAA-bound CS1; and (F) α-KG- and PC-bound CS1. Figures were generated from PDB IDs 1IPS, 1BK0, 1RXG, 1DS1, 1DRY, and 1DRT using software Rasmol. Metal ions, side chains of protein ligands of the metal ions, substrates, cosubstrate, and water molecules are shown as balls and sticks. Mn atom is in dark gray. Fe atoms are in golden yellow. Substrates (ACV in B, NAA in E, and PC in F) are in yellow. Cosubstrate α-KG is in green. Protein ligands of the metal ions are in blue. Coordinated water molecules are in red. Noncoordinated water molecules are in pink. Protein backbone is in magenta. All other atoms are shown in light lines. Coordination bonds shown in solid black lines; hydrogen bonds shown in dashed black lines. The perspective is the metal-distant histidine bond, which is almost perpendicular to the plane of the paper, while the carboxylate ligand is on the top and the proximal histidine is on the left.

oxygen of the monodentate iron ligand in the structure of the two α-KG-dependent enzymes, DAOCS and CS1, as well as IPNS, which may play an important role in stabilizing the coordinated water (see Figure 7A−E).[60] Further (co)substrate binding can affect this internal hydrogen bond. From Figure 7E,F, in the structures of CS1/Fe^{II}/α-KG/NAA and CS1/Fe^{II}/α-KG/PC, the acetyl group of the substrate analogue NAA and the monocyclic β-lactam ring of the substrate PC are in van der Waals contact with Oϵ of Glu146. Therefore, the binding of the substrate can affect the conformation of the side chain of Glu146, interfering with the internal hydrogen bond to the bound water. In fact, in the structure of CS1/Fe^{II}/α-KG/PC the carboxylate plane is rotated away from the normal (38°) more than in CS1/Fe^{II}/α-KG (33°) or CS1/Fe^{II}/α-KG/NAA (28°). This reduces or eliminates an important hydrogen-bonding interaction and could contribute to the loss of the water. The acetyl group of the substrate analogue NAA is less rigid, which is consistent with the fact that the water is not lost but is at a longer distant from the ferrous center.

(60) In IPNS/Fe^{II}/ACV, there is a hydrogen-bonding interaction between the uncomplexed Oδ atom of Asp216 and the water trans to His214 (proximal His). In DAOCS/Fe^{II}/α-KG, the coordinated water hydrogen bonds with the uncomplexed Oδ of Asp185. In CS1/Fe^{II}/α-KG, the coordinated water is trans to His279 (distant His), and the Oϵ of Glu146 is still in a good position to hydrogen bond to the water.

Molecular Mechanism for the Uncoupled Reaction. The five-coordinate ferrous species in the presence of both cosubstrate and substrate is critical for the coupled reaction of CS2 and perhaps all the α-KG-dependent non-heme iron enzymes.[40] In the absence of substrate, an uncoupled reaction in which the α-KG is decarboxylated occurs at a rate that is a few percent of that of the coupled reaction.[29−34] From CD, MCD, and VTVH MCD, in the absence of substrate, the CS2/Fe^{II}/α-KG complex is pure six-coordinate with α-KG bound to the iron.[39] Thus, the reaction of α-KG is promoted by Fe^{II} coordination, but a six-coordinate ferrous species is involved in the uncoupled reaction in the absence of substrate. The O_2 must compete with the bound water for the iron site; thus, the reaction rate is very slow. This reaction would activate dioxygen for attack of the α-keto carbon, leading to the oxidative decarboxylation of α-KG and the possible generation of an oxo-ferryl intermediate. In the absence of substrate, this intermediate may oxidize a nearby protein residue, resulting in a deactivated enzyme. Substrate analogues, which bind in a similar manner as the substrate, but cannot be hydroxylated or oxidized, would induce the six- to five-coordination conversion and accelerate the rate of uncoupled reaction as observed from some of the α-KG-dependent enzymes (e.g., prolyl 4-hydroxylase, lysyl hydroxylase, [35,36] and γ-butyrobetaine hydroxylase[37]). Interestingly, the uncoupled

reaction occurs even in the presence of substrate for most of the α-KG-dependent enzymes, including CS2, as evidenced by the facts that the amount of decarboxylation product CO_2 exceeds the hydroxylation (oxidation) product and that the enzymes are slowly deactivated.[15,37] For CS2, when PC is the substrate, the rate of enzyme inactivation (which is related to the rate of the uncoupled reaction[61]) in the presence of substrate is about one-third of the rate in the absence of substrate.[15] From CD, MCD, and VTVH MCD studies of the CS2/Fe^{II}/α-KG/PC complex, approximately 10% of the sites remain six-coordinate with substrate PC bound. The facts that both the rate of the uncoupled reaction and the amount of six-coordinate species are significantly decreased in the presence of substrate PC are consistent with the proposal that the six-coordinate ferrous species catalyzes the uncoupled reaction in the presence of substrate. In the six-coordinate ferrous species, the substrate may bind in a different conformation such that it is not efficiently hydroxylated (oxidized) by the possible oxo-ferryl intermediate, which would lead to deactivation of the protein.

Structure/Reactivities Correlations. From these MCD and VTVH MCD studies, CS2 is converted by the binding of each of the three substrates into a similar five-coordinate species, which would catalyze the coupling of the oxidative decarboxylation of α-KG with three different types of oxidative reactions: hydroxylation of DGPC, oxidative ring closure of PC, and desaturation of dihydroclavaminic acid and DPC. Insight into the structural origin of these different reactivities comes from the recent CS1/Fe^{II}/α-KG crystal structures with the hydroxylation substrate DGPC analogue NAA and the ring-closure substrate PC bound in the substrate-binding pocket.[38] The guanidine and carboxylate groups of the bound NAA have extensive electrostatic and hydrogen-bonding interactions, with the amino acid side chains and peptide backbone lining the substrate binding pocket. This orientation projects its 3-(*pro-R*) C−H bond, which is to be oxidized, toward the water coordinated to the iron.[38] The binding mode of PC is only slightly different from that of NAA, with its amine group less rigidly bound. The hydroxyl group is closest to the open coordination position with an O−Fe^{II} distance of 4.20 Å.

The generally considered molecular mechanism of α-KG-dependent non-heme iron enzymes invokes an oxo-ferryl species, which results from the nucleophilic attack of the activated dioxygen on the α-keto group of α-KG and the subsequent collapse of the bridged peroxo species.[3,24] The oxo-ferryl intermediate would then abstract the hydrogen atom from a nearby C−H bond of the substrate (RH_2), generating a substrate radical (•RH) and a ferric hydroxide species (Scheme 2). The cosubstrate product succinate may bind to the iron in a bidentate mode. At this stage, the reactivity of the resultant ferric hydroxide species would branch to either the hydroxylation or the ring-closure (or desaturation) reaction (Scheme 2). The hydroxylation reaction mechanism would involve a rebound step which can be considered to be a homolytic cleavage of the Fe^{III}−OH^- bond, giving a five-coordinate ferrous species and a hydroxyl radical, which then combines with the substrate radical, forming the hydroxylation product (HORH). Alternately, the oxidative ring-closure and desaturation reaction involves a second hydrogen atom abstraction step by the ferric hydroxide

Scheme 2

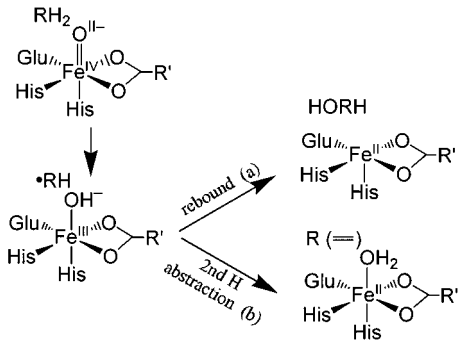

species, similar to the hydrogen abstraction step in the lipoxygenase reaction.[62] This would result in a six-coordinate ferrous species and a substrate diradical, which would then form either a ring or a double bond (R). Due to the complication of ring strain in the ring-closure reaction, the following discussion considers only the desaturation (and hydroxylation) reaction.

The driving force of the rebound step (branch a) is related to the strength of the C−OH bond produced and the Fe^{III}−OH^- bond broken, which through a Born scheme is related to the Fe^{III}/OH^- interaction energy and the reduction potential of the five-coordinate Fe^{III}/Fe^{II} couple: the lower the Fe^{III}−OH^- interaction energy, the larger the driving force for the rebound step. [63] The driving force of the second hydrogen atom abstraction step (branch b) is related to the strength of the O−H bond produced in the six-coordinate ferrous species, the diradical reorganization energy (in the case of desaturation, this equals the π bond strength), and the strength of the C−H bond broken in •RH. A Born scheme relates the driving force of this reaction to the pK_a of water complexed to six-coordinated ferrous species and the reduction potential of the six-coordinate Fe^{III}/Fe^{II} couple: the higher the pK_a of the ferrous bound water, the higher the driving force for the second hydrogen abstraction step.[64]

The difference in the ability of the ferric hydroxide species to carry out the rebound reaction versus the second hydrogen atom abstraction can be estimated from the difference of the heats of formation of the products of the two reactions, i.e., the heat of formation of the hydroxyl product plus a five-coordinate ferrous species and that of the desaturation product plus a six-coordinate ferrous species with water bound. A simplified model is considered which compares the heat of formation of 2-butanol and 2-butene plus water and its interaction energy with a five-coordinate ferrous species (E(water−Fe^{II}_{5C})). The product of hydroxylation (2-butanol) is more exothermic (−70 kcal mol^{-1}) than the product of the desaturation (2-butene and water, (−2) + (−58) = −60 kcal mol^{-1}), which shows that the rebound reaction is more favored than the second hydrogen atom abstraction, not including the contribution from E(water−Fe^{II}_{5C}) in the latter step. E(water−Fe^{II}_{5C}) can be correlated to the thermodynamic parameters of the individual steps (vide supra), which gives an estimation of E(water−Fe^{II}_{5C}) of approximately −14 kcal mol^{-1},[65] comparable to the heat of formation difference. The larger the value of E(water−Fe^{II}_{5C}), the more likely the water will stay bound at the ferrous site, which favors the second hydrogen atom abstraction over the rebound reaction in

(61) In the absence of external reductants, e.g., ascorbic acid, the rate of enzyme deactivation should equal the rate of the uncoupled reaction, since that would lead to oxidization of the active site. However, the deactivation rate is measured in the presence of ascorbic acid, and under these conditions, the rate of enzyme deactivation would be decreased by the ascorbate-dependent reduction of the oxidized active site.

(62) Solomon, E. I.; Zhou, J.; Neese, F.; Pavel, E. G. *Chem. Biol.* **1997**, *4*, 795−808.

(63) $\Delta G°$(rebound) = $\Delta G°$(OH^-−Fe^{III}) − 23.1$E°$(5C,Fe^{III}/Fe^{II}) − 45 (kcal mol^{-1}).

(64) $\Delta G°$(2nd H abstraction) = −11 − 1.36pK_a − 23.1$E°$(6C,Fe^{III}/Fe^{II}) (kcal mol^{-1}).

Scheme 2. Therefore, we hypothesize that the protein could also *contribute* to the reactivities of the ferric hydroxide species to carry out either the rebound reaction or the second hydrogen atom abstraction by regulating $E(\text{water}-\text{Fe}^{\text{II}}_{5\text{C}})$ in the enzyme−product complex. As presented above, MCD and VTVH MCD studies of the enzyme−substrate complex CS2/Fe^{II}/α-KG/DPC show the presence of the highest amount of six-coordinate water-bound species, consistent with that fact this complex mostly undergoes the desaturation reaction. Alternatively, for DGPC a dominant five-coordinate species is present with substrate bound, indicating a low value of the water−$\text{Fe}^{\text{II}}_{5\text{C}}$ interaction energy, thus favoring the rebound and hydroxylation reaction. While the energetics considered above involves the strength of the water−Fe^{II} bond in the product complex, the MCD data do show that this bond strength can be affected by the different substrates.

(65) $E(\text{water}-\text{Fe}^{\text{II}}5\text{C}) = -23.1[E°(6\text{C},\text{Fe}^{\text{III}}/\text{Fe}^{\text{II}}) - E°(5\text{C},\text{Fe}^{\text{III}}/\text{Fe}^{\text{II}})] - 1.36[(\text{p}K_a(\text{water}) - \text{p}K_a(\text{water}-\text{Fe}^{\text{II}})] + \Delta G°(\text{OH}^-\text{−Fe}^{\text{III}}) = -14$ kcal mol^{-1}, in which the first term is the reduction potential difference of a six- and five-coordinate iron site (estimated at about −0.5 V), the second term is the pK_a difference of a free and Fe^{II}-coordinated water (estimated at about −4.5 log units) (Baes, C. F., Jr.; Mesmer, R. E. *The Hydrolysis of Cations*; Wiley: New York, 1984; Chapters 10, 12, and 13), and the third term is the $\text{Fe}^{\text{III}}-\text{OH}^-$ interaction energy (estimated at about −32 kcal mol^{-1}) (Sawyer, D. T. *Oxygen Chemistry*; Oxford University Press: New York, Oxford, 1991).

Summary

Our studies of the CS2 interaction with three substrates having different reactivities provide significant molecular level insight into the structure/function correlations of this multifunctional enzyme. α-KG binds to a six-coordinate Fe^{II}, promoting its uncoupled decarboxylation. Varying amounts of six-coordinate ferrous species in the substrate complexes may be correlated to the uncoupled reaction in the presence of substrate. Similar five-coordinate species are present for all three substrate complexes with α-KG bound, which appears to be critical for the coupling of the oxidative decarboxylation of α-KG to the different oxidative reactions of the substrates. A hypothesis is considered that the enzyme may contribute to the type of reactivity by regulating the binding energy of water to the five-coordinate ferrous species in the enzyme/succinate/product complex. A weakly bound water would favor the rebound mechanism and thus the hydroxylation reaction, while a higher $\text{Fe}^{\text{II}}-\text{OH}_2$ bond strength would favor the second hydrogen atom abstraction mechanism and thus ring closure or desaturation.

Acknowledgment. This research was supported by grants from the National Institutes of Health (GM40392, E.I.S., and AI14937, C.A.T.).

JA004025+